NUCLEAR SCIENCE AND ENGINEERING · VOLUME 187 · 127–141 · AUGUST 2017

DOI: http://dx.doi.org/10.1080/00295639.2017.1301739

Impact of ^{235}U Resonance Parameter Evaluation in the Reactivity Prediction

Luiz Leal,[a]* Adimir Dos Santos,[b] Evgeny Ivanov,[a] and Tatiana Ivanova[c]

[a]*Institut de Radioprotection et de Sûreté Nucléaire (IRSN), PSN-EXP/SNC, Fontenay-aux Roses 92262, France*
[b]*Cidade Universitaria, Instituto de Pesquisas Energéticas e Nucleares – IPEN/CNEN-SP, Av. Prof. Lineu Prestes 2242, Sao Paulo 05508-000, Brazil*
[c]*OECD Nuclear Energy Agency (NEA), 46 Quai Alphonse Le Gallo, Boulogne-Billancourt 92100, France*

Received January 23, 2017
Accepted for Publication February 26, 2017

Abstract — *Resonance parameter evaluation of the ^{235}U cross sections using the Reich-Moore formalism was done with the computer code SAMMY from 0 to 2.25 keV to address issues with capture cross-section and standard fission cross-section values. The evaluation includes recent capture and fission cross-section measurements as well as high-resolution data used in previous ^{235}U evaluation. Moreover the new ^{235}U resonance parameter evaluation has been used in the calculation of a new benchmark experiment performed at the IPEN/MB-01 research reactor. The experiment, named the inversion point of the isothermal reactivity coefficient, is used to test temperature effects at low temperature. The results demonstrate that the new ^{235}U evaluation has greatly improved the prediction of reactivity temperature coefficient in contrast to previous evaluations. This paper is outlined in two parts, namely the first part deals with the description of the ^{235}U resonance analysis and evaluation up to 2.25 keV, and the second part presents the results of the isothermal reactivity coefficient calculations performed on the IPEN/MB-01 reactor.*

Keywords — *Resonance, evaluation, benchmark.*

Note — *Some figures may be in color only in the electronic version.*

I. INTRODUCTION

Neutron cross sections of fissile elements cannot be described by a formalism that does not account for the asymmetries observed in the resonances of the reaction cross section. In the late 1980s and early 1990s a ^{235}U Reich-Moore resonance evaluation was performed from thermal to 2.25 keV (Ref. 1) using the SAMMY code.[2] It was the first attempt to use a more rigorous resonance formalism to address issues with interference effect in the fission channels. The evaluation represented an improvement compared to previous ^{235}U evaluations for which the Single-Level Breit-Wigner (SLBW) formalism was used together with background cross sections to make up for the SLBW deficiency to represent fissile isotope. The use of the Reich-Moore formalism for resonance parameter representation was a major change for the ENDF. Hence, a decision was made by the Cross Section Evaluation Working Group (CSEWG) to start a new ENDF series which was named the ENDF/B-VI. The first released version was the ENDF/B-VI.1. In contrast to the effort for generating the ENDF/B-VI.1 differential data evaluation, the integral benchmark testing was not sufficient to thoroughly assess the evaluation effectiveness prior to its inclusion in the evaluated files. The evaluation was adopted in evaluated nuclear data projects and then underwent a series of benchmark testing. The testing included sensitivity analysis and cross-section adjustments based on benchmark experiments. The results demonstrated that the evaluation performed poorly mainly due to concerns with the capture cross section in

*E-mail: luiz.leal@irsn.fr

the energy region 22.6 to 454 eV (Ref. 3), indicating a need for increasing the capture cross section. However no issue with the fission cross section was found. A close inspection of the problem reviewed that a low value of the average gamma-capture width was responsible for the very low-capture cross section. It should be pointed out that no reliable capture cross-section measurements existed at the time in the energy range above 100 eV. There existed capture cross-section data but these data were not systematically included in the evaluation due to issues such as normalization and background. Hence the ^{235}U was revised on the basis of integral results and sensitivity analysis. The revised ^{235}U evaluation was made available in the ENDF, JEFF, and JENDL projects. The ENDF release, including the revised ^{235}U resonance parameter evaluation, was named ENDF/B-VI.4. A detailed description of the ^{235}U evaluation is given in Ref. 4. The JENDL project adopted the evaluation up to 500 eV and used an unresolved resonance representation above 500 eV to help improve the results of the fast critical assembly benchmark (FCA) (Ref. 5). The revised evaluation gave a high-capture cross section that did not support the FCA benchmark results. A similar scenario observed with the FCA benchmark calculations was also observed with the ZEUS benchmark. These divergences with integral benchmark calculations prompted the proposal for a subgroup of the Working Party on International Nuclear Data (WPEC) to investigate the ^{235}U capture problem.[6] The results of the WPEC criticality calculations showed an overestimation of the ^{235}U capture cross section of about 10%. The WPEC recommendation was that rather than re-evaluating the ^{235}U resonance parameters based solely on integral benchmark results, new capture cross-section measurements should be made to confirm the findings of the WPEC subgroup. Hence, time-of-flight (TOF) capture cross-section measurements were planned and performed independently at the Rensselaer Polytechnic Institute (RPI) (Ref. 7) and at the Los Alamos National Laboratory (LANL) (Ref. 8). These new measurements were used together with the computer code SAMMY to update the ^{235}U resonance parameters in the energy range from thermal to 2.25 keV. The results demonstrated an improvement in benchmark calculations. However, despite all efforts to address the capture issue in the resonance region, the problem with the fission standard cross section still remained. Recently measured fission cross-section data carried out at the n_TOF machine located at the European Organization for Nuclear Research (CERN) in Geneva provided strong support to the fission standard values. Indeed, normalization of the n_TOF fission cross-section data in the energy range 7.8 to 11.0 eV supported the standard value in this energy range but also reinforced the standard averaged fission cross-section values in the resonance region above 100 eV. Hence, the resonance parameter evaluation was revised with the inclusion of the n_TOF experimental fission data.

II. ^{235}U RESONANCE EVALUATION IN THE ENERGY RANGE 10^{-5} eV TO 2250 eV

II.A. External Energy Level Determination

An accurate representation of the external resonance contributions is essential for the fitting of the experimental data. For instance, the long-range interference effects inherent in the R-matrix methodology preclude finding a good fitting of the experimental fission data if the external resonance contributions are not properly taken into account. The external resonance levels are meant to reproduce the interference effects of resonances below 0 eV and above 2250 eV in the energy range 0 to 2250 eV. An infinite number of energy levels exist. However a truncated set of 10 external energy levels—five below 0 eV (bound levels) and five above 2250 eV—were determined to mockup the effect of the numerous energy levels. The bound levels contain a negative energy close to 0 eV, with a very small neutron width that is responsible for the bending of the energy dependence of the η(E)(eta) at low energy[9] that leads to an improved calculation of the Doppler reactivity effects. They are listed in Table I for which each resonance is described by the resonance energy E_r, gamma width Γ_γ, neutron width Γ_n, two fission widths Γ_{f1} and Γ_{f2}, and the spin and parity J^π. An accurate representation of the external resonance contribution provides the grounds to determine the effective scattering radius. The analysis of high-resolution transmission data led to an effective scattering radius of 9.602 fm following a similar procedure as explained in Ref. 4.

II.B. Experimental Data Base

The main features of the new resonance parameter evaluation are the addition of new cross-section measurements done at LANL, RPI, and the n_TOF. Capture cross-section measurements done at LANL and RPI were central to unveil issues with the capture cross section above 100 eV. The fission cross-section measurements carried out at n_TOF supported the standard cross-section values. Furthermore, the evaluation was done including high-resolution

TABLE I

Energy Bound Levels and Energies Above 2.25 keV

	E_r (eV)	Γ_γ (meV)	Γ_n (meV)	Γ_{f1} (meV)	Γ_{f2} (meV)	J^π
Energy bound levels	−75.405	47.781	507.274	−487.090	−443.345	3^-
	−5.253	36.797	12.170	195.681	−160.038	4^-
	−0.481	39.228	0.088	129.661	−80.535	3^-
	−0.432	38.024	0.033	167.072	−8.283	4^-
	-3.657×10^{-5}	39.988	6.461×10^{-8}	−0.509	0.935	4^-
Energy levels above 2.25 keV	2281.325	44.083	12.459	155.711	458.850	4^-
	2284.014	41.147	3802.461	1956.501	22.864	3^-
	3312.563	47.228	11457.530	474.421	571.292	3^-
	3819.129	38.494	1242.316	−511.662	67.709	4^-
	4500.997	33.681	33.8.548	286.623	364.141	3^-

transmission, fission cross-section, and eta measurements that were accounted for in previous ^{235}U evaluations. The experimental data used in the resonance parameter evaluation are displayed in Table II in which TOF is indicated by L, thickness by n, and temperature by T. The Reich-Moore approach of the SAMMY code was used for fitting the

TABLE II

Experimental Data Included in the SAMMY Resonance Analysis

Reference	Energy Range (eV)	Data
Transmission		
Harvey et al.[10] (ORNL/1986)	0.4 to 68.0	L = 18 m, n = 0. 03269 atom/barn, and T = 77 K
Harvey et al.[10] (ORNL/1986)	4.0 to 2250.0	L = 80 m, n = 0. 00233 atom/barn, and T = 77 K
Harvey et al.[10] (ORNL/1986)	4.0 to 2250.0	L = 80 m, n = 0. 03269 atom/barn, and T = 77 K
Spencer et al.[12] (ORNL/1984)	0.01 to 8.0	L = 18 m, n = 0.001468 atom/barn, and
Fission		
Gwin et al.[37] (ORNL/1984)	0.1 to 20.0	L = 25.6 m and T = 293.6 K
Weston and Todd[14] (ORNL/1992)	100.0 to 2250.0	L = 86.5 m and T = 293.6 K
Weston and Todd[38] (ORNL/1984)	14.0 to 2250.0	L = 18.9 m and T = 293.6 K
Paradela et al.[13] (n_TOF/2010)	0.7 to 1000.0	L = 185 m and T = 293.6 K
Danon[7] (RPI/2011)	100.0 to 2250.0	Yield
		L = 25.56 m, n = 0. 004357 atom/barn, and T = 293.6 K
Wagemans et al.[39] (Geel/1988)	0.001 to 0.4	L = 18 m and T = 293.6 K
Eta		
Wartena et al.[40] (Geel/1987)	0.0018 to 1.0	L = 8 m and T = 293.6 K
Weigmann et al.[35] (ILL/1990)	0.0015 to 0.15	Chopper, T = 293.6 K
Moore et al.[16] (ORNL/1978)	1.6 to 100	L = 13.4 m and T = 293.6 K polarized neutron and polarized target
Capture		
Danon[7] (RPI/2011)	100.0 to 2250.0	Yield
		L = 25.56 m, n = 0. 004357 atom/barn, and T = 293.6 K
Jandel et al.[8] (LANL/2012)	100.0 to 2250.0	L = 25.45 m and T = 293.6 K
Perez et al.[15] (ORNL/1973)	0.01 to 200.0	L = 39.7 m and T = 293.6 K
De Saussure et al.[41] (RPI/1967)	0.01 to 2250.0	L = 25.2 m and T = 293.6 K

data. A total of 3170 resonance levels were identified in the energy range 0 to 2250 eV to reproduce the experimental data within the data uncertainty. The spin-separated fission data were used below 100 eV to verify the resonance spin assignment. The data correspond to fission cross-section measurements done at the Oak Ridge Electron Linear Accelerator (ORELA) for the two s-wave spin states $J = 3^-$ and $J = 4^-$. The total cross-section fitting was based on the high-resolution transmission data taken at ORELA by Harvey et al.[10] A consistent SAMMY sequential Bayes' fitting was carried out using the experimental data listed in Table II. The procedure has allowed the generation of resonance parameter covariance which is not a topic involved in the present paper.

II.C. ^{235}U Resonance Parameter Evaluation

The ground state spin and parity of the ^{235}U target is $\frac{7^-}{2}$ and $\frac{1^+}{2}$ for the incident neutron, leading to two possibilities for the channel spins which are $s = 3^-$ and $s = 4^-$. The total angular momentum for the compound nucleus will assume values between $|l - s|$ and $|l + s|$ where l is the relative neutron-nucleus angular momentum which values define the s-wave for $l = 0$, p-wave for $l = 1$, etc. For the evaluation performed in this work, it was assumed that all the resonances observed were s-wave. Table III shows the p-wave penetrability as a function of energy, for four energies relative to the s-wave penetrability. It may happen that few portions of the observed resonances are p-wave and also that some small p-wave resonances are missing. These p-wave resonances were not identified in the experimental data base used. However the sole use of s-wave has not prevented obtaining a good fit of the experimental data.

The values displayed in the second column of Table III are calculated with $\rho^2 = 3.321 \times 10^{-6}E$, where E is the incident neutron energy in eV.

TABLE III

p-wave ($l = 1$) Penetrability Factor Relative to the s-wave ($l = 0$) Penetrability Factor $p_0 = \rho$

Energy (eV)	$\frac{p_1}{p_0} = \frac{\rho^2}{\rho^2+1}$
1	3.32×10^{-6}
100	3.32×10^{-6}
500	1.66×10^{-3}
1000	3.31×10^{-3}
2000	6.60×10^{-3}

Before starting the fitting of the data shown in Table II, a careful examination of the experimental conditions was done. Experimental resolution, normalization, background, multiple-scattering, data alignment, etc., were inspected to assure consistency with the data set. A sequential analysis of the data shown in Table II was carried out with the SAMMY code to achieve a reasonable fit of the data with an acceptable χ^2. Not only the resonance parameters were let to vary, but also normalization, resolution parameters, etc., were also searched.

The two experimental $\eta(E)$ values at the low energy were fitted with the SAMMY code. The $\eta(E)$ shape observed in the experimental is followed by the fitting of the data. The bending effect perceived is the result of the interference effects of the bound level placed at the energy -3.657×10^{-5} eV with a very small neutron width. The fitting is displayed in Fig. 1. The $\eta(E)$ shape at low energy dictates the improvements on the calculated reactivity temperature coefficient as will be seen in Sec. III. The standard recommended number of neutrons per fission at thermal (0.0253 eV) of 2.4257 was used in the $\eta(E)$ calculation.

The fitting of the cross section at low energy provided a good representation of the thermal cross-section values in good agreement with the standard indicated values.[11] The values are listed in Table IV.

Also listed in Table IV are the ENDF/B-VII.1 thermal values. The ENDF/B-VII.1 thermal capture is lower than the standard value by about 0.64%, the scattering is higher by about 7.27%, and the fission cross sections are essentially the same. The impact of these differences in the calculation of the Doppler reactivity effects will be discussed in Sec. III.B. Fitting of the n_TOF fission cross-section data was

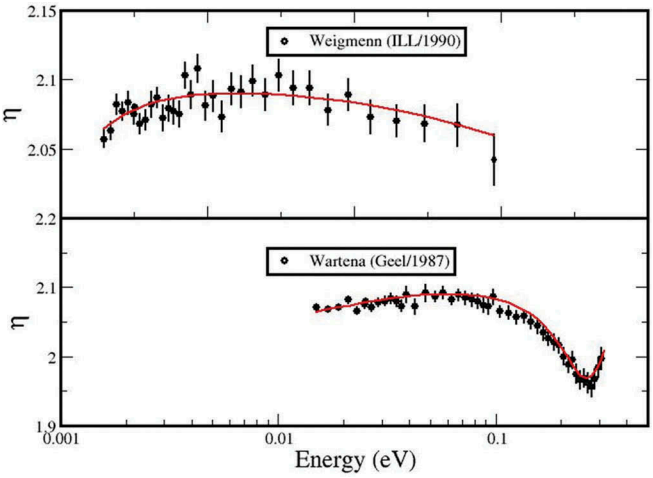

Fig. 1. Comparison of the experimental and calculated $\eta(E)$ in the thermal energy range.

TABLE IV

Standard Values and Resonance Parameter Results

Parameter	Standard Values (barns)	Values Obtained with the New Resonance Parameter Evaluation (barns)	ENDF/B-VII.1 (barns)
σ_f	584.4 ± 1.0	584.4 ± 4.2	584.897
σ_γ	99.3 ± 0.7	99.2 ± 3.1	98.664
σ_s	14.1 ± 0.2	14.1 ± 0.8	15.112

performed in the energy range 0.7 to 2250 eV. The n_TOF fission data were normalized in the energy range 7.8 to 11 eV according to the standard value in this energy range which is 246.396 ± 1.244 b.eV. Rather than fitting the normalized fission data, a decision was made to use the data without the normalization and to include the standard fission integral value in the fitting process as part of the experimental data for the SAMMY code. It was noted that, as a result of this procedure, the average values of the fission cross section related to the standard were straightforwardly fitted. The 7.8 to 11 eV calculated fission integral obtained with the resonance parameters is 246.854, which is in good agreement with the standard values

The results of the fitting of Harvey et al.,[10] Spencer et al.,[12] and Paradela et al.[13] are shown in Fig. 2. An examination of the transmission data of Harvey revealed an inconsistency with the remaining data set around the energy 4.25 eV. It was discovered that the issue was due to an impurity of ^{181}Ta present in the target sample. Although the data reduction was

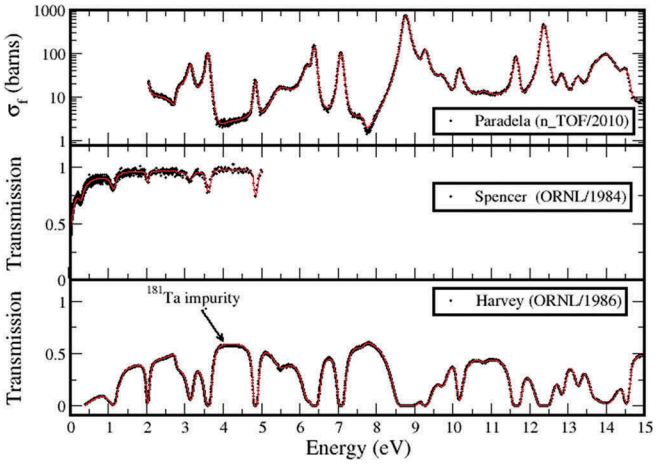

Fig. 2. Comparison of the SAMMY fit of the experimental data.

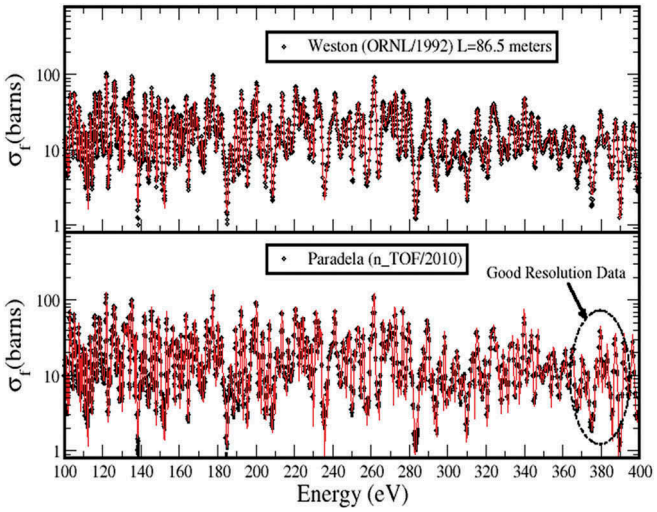

Fig. 3. SAMMY fitting of the fission cross-section data of Weston and Todd[14] and Paradela et al.[13] in the energy range 100 to 400 eV.

suitably done, it appears that the ^{181}Ta impurity was not completely removed.

It is interesting to note that the fission integral value in the energy region 7.8 to 11.0 eV led to a normalization of the Weston and Gwin fission data of about 2%. The fitting of the Weston and Todd[14] and Paradela et al.[13] is shown in Fig. 3 in the energy range 100 to 400 eV. The resolution of the n_TOF data is excellent, displaying the details of the Porter-Thomas–like fluctuations not seen in the Weston data at this energy range as indicated in the oval.

Two measured capture data at LANL and RPI, respectively, were used in the resonance evaluation above 100 eV. The capture data of Perez et al.[15] were used below 200 eV. The three data sets are displayed in Fig. 4 together with SAMMY fit in the energy range 100 to 200 eV. As can be seen, the resolution of the RPI data is excellent for use in the resonance analysis. The TOF lengths for the three measurements are about the same, with the main difference on the neutron burst width. In the energy range 100 to 200 eV the SAMMY fit was based on the Perez et al.,[15] Danon,[7] and Jandel et al.[8] capture data. Above 200 eV the fitting relied mainly on the RPI data.

II.D. Average Resonance Parameters Values

Average values of the ^{235}U resonance parameters were determined in the energy up to 100 eV for 207 resonances using the SAMDIS module of the SAMMY code system.[2] The SAMMY fitting of the spin-separated fission cross section[16] for the $J = 3^-$ and $J = 4^-$ states in the energy range 2 to 100 eV is shown in Fig. 5. The high-resolution transmission data, fission cross-section

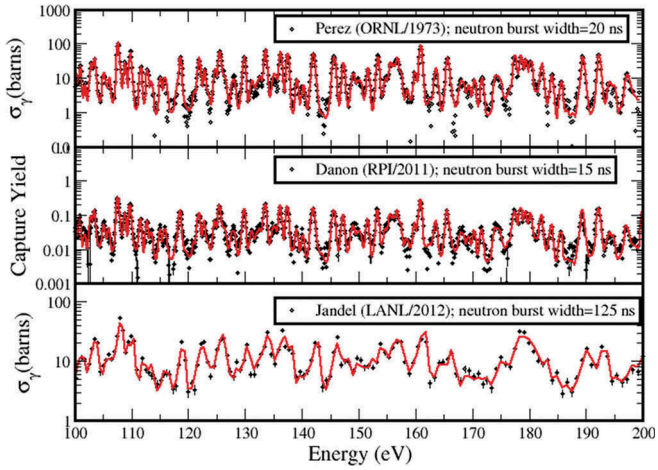

Fig. 4. Comparison of the SAMMY fit of the capture data.

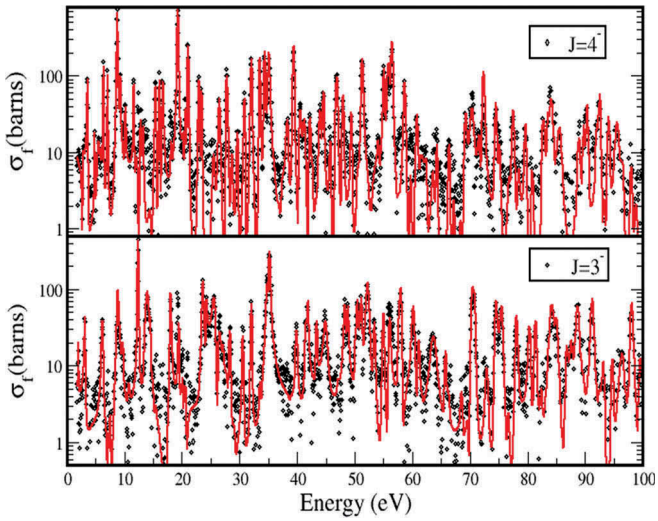

Fig. 5. SAMMY fitting of the spin-separated fission cross section of Moore et al.[16]

data, and the spin-separated fission data have allowed resolving the majority of resonances up to 100 eV, providing a good estimation of the average values of the resonance parameters.

The average values for the total angular momentum $J = 3^-$ and $J = 4^-$ are presented in Table V. They correspond to the average of energy level spacing, s-wave strength function, average of fission width, and gamma capture average.

III. TESTS OF THE NEW ^{235}U RESONANCE PARAMETER EVALUATION ON REACTIVITY PREDICTIONS

Tests of the new ^{235}U resonance parameter evaluation were done using very recent integral benchmark

TABLE V

Average Value of ^{235}U Resonance Parameters Up to 100 eV

	$J = 3^-$	$J = 4^-$
Energy level spacing (eV)	1.13 ± 0.07	0.83 ± 0.04
s-wave strength function ($\times 10^4$)	0.84 ± 0.05	0.96 ± 0.05
Fission width (meV)	269.3 ± 51.8	158.2 ± 15.8
Gamma capture width (meV)	40.0 ± 0.9	39.5 ± 0.8

measurements carried out at the IPEN/MB-01 reactor[17] that have been accepted for inclusion in the IRPhE handbook. This new benchmark is named the inversion point of the isothermal reactivity coefficient of the IPEN/MB-01 reactor. The main reasons for this choice are given in the following paragraphs.

Several studies[18,19] made with the IPEN/MB-01 reactor core configuration suggested a very high sensitivity of the isothermal reactivity coefficient to the shape and magnitude of the thermal ^{235}U cross sections. The IPEN/MB-01 facility has quite a few unique features that favor the neutron thermal energy region. Several calculated responses have been found to be very sensitive to the thermal nuclear data, particularly to those of ^{235}U. The intent of this paper is to describe how the isothermal reactivity coefficient has been used to test the new ^{235}U cross-section evaluation. The inversion point of the isothermal reactivity coefficient is by definition the temperature where the reactor response becomes positive. The inversion point has similar sensitivity trends to the thermal and subthermal ^{235}U cross sections as the isothermal reactivity coefficient of the IPEN/MB-01 reactor does. Such quantity will provide excellent grounds for testing the new ^{235}U resonance parameter evaluation regarding the reactor temperature evolution. The inversion point has been found to be an adequate experimental quantity that is used to validate methodologies and nuclear data libraries for reactivity coefficient determination. Its experimental determination does not require any sort of computed correction factors or any quantity that comes either from calculations or from another experiment. By contrast, the isothermal reactivity coefficients are not a directly measured quantity but rather they are constructed on the basis of the experimental determination of the reactivity. The reactivity between two points at different temperature is not measured directly; rather it is inferred by employing a reactivity meter together with a set of delayed neutron parameters. These parameters are obtained either by numerical approach or by experiments.

However, the delayed neutron parameters are physical quantities of very difficult experimental or numerical determination which will impose restrictive uncertainty on the isothermal reactivity coefficient. The proposed experimental quantity employed here will avoid this sort of difficulty. The inversion point of the isothermal reactivity coefficient of the IPEN/MB-01 reactor constitutes a very stringent test for the ^{235}U nuclear data. Three configurations will be employed for the new ^{235}U resonance parameter test.

III.A. Facility Description

The IPEN/MB-01 reactor is a zero power critical facility specially designed for measurements of a wide variety of reactor physics parameters to be used as experimental benchmark data for checking the efficiency of nuclear data libraries commonly used in reactor analysis and design. The IPEN/MB-01 reactor reached its first criticality on November 9, 1988, and since then it has been utilized for basic reactor physics research and as part of a laboratory system for academic purposes. The facility consists of a 28 × 26 square array of UO_2 fuel rods 4.3% enriched and cladded by stainless steel (SS-304) inside a light water tank. The control banks are composed of 12 Ag-In-Cd rods and the safety banks of 12 B_4C rods. The pitch of the IPEN/MB-01 reactor was chosen to be close to the optimum moderator ratio (maximum k_∞). This feature favors the neutron thermal energy region events, and at the same time provides the isothermal reactivity coefficient of the IPEN/MB-01 reactor core with an inversion point. This facility has a well-defined geometric and material data composition. Many experiments carried out at the IPEN/MB-01 reactor have been included in international benchmark handbooks for several critical configuration experiments[20,21] and several other classical reactor physics experiments.[22] Additional information regarding the IPEN/MB-01 reactor and facility is available in benchmark reports LEU-COMP-THERM-077 (Ref. 20) for the standard core and LEU-COMP-THERM-044 (Ref. 20) for the core with stainless steel rods.

III.B. Benchmark Description

The benchmark experiments were based on the standard 28 × 26 fuel rod configuration as shown in Fig. 6. Three configurations were employed for the test of the new ^{235}U resonance parameters. The differences among them reside in the central region of the core. Configuration A considers the central region filled with fuel rods. Configuration B considers the central region filled with SS-304 rods. The SS-304 rods are the same as those described in LEU-COMP-THERM-044. Configuration C considers the central region filled with water. The experiments[23,24] proceeded in the following way: Instead of heating the reactor system, as is usual in experiments considering temperature variation, the reactor system is cooled down. The initial temperature and its range vary from configuration to configuration. For example, for configuration A the water was cooled down to ~8.5°C. Employing the heating/cooling system of the facility, the temperature is allowed to increase in a stepwise manner. For each step, the reactor system is allowed to reach thermal equilibrium. The BC1 control bank is always kept in a fixed position while the fine adjustment to reach criticality is performed by continuously adjusting the axial position of the BC2 control bank. The temperature and the critical control bank axial positions for each step are recorded for further analysis. The inversion point of the isothermal reactivity coefficient is inferred by fitting the BC2 critical control bank position as a function of the temperature based on a second order polynomial function. The inversion point is the temperature where the minimum of such curve occurs.

The final evaluated results for the inversion point are shown in Table VI. The final total uncertainties (1σ) combine the geometric and material uncertainties and the experimental uncertainties.

The experimental results on the inversion point of the isothermal reactivity measurements can be used for testing the ^{235}U cross sections in the low energy range. In addition, one should note that the shape of the cross section in the low energy region is intimately correlated with entire resonance region. Hence the nuclear data evaluation test on the basis of the isothermal reactivity measurements impacts the thermal and epithermal energy ranges. The shape of the ^{235}U fission and capture cross sections below 5 eV is displayed on Fig. 7. Another interesting point to note is that the shift in the neutron spectrum due to the neutron thermalization provides essentials for testing the thermal neutron scattering models. This item is not a part of the present work. The shift in the neutron spectrum is due to the fact that the actual neutrons effective temperature is larger than the nominal reactor temperature.[25] The variations of the neutrons effective temperature drives the reactivity swing due to the shape of the ^{235}U fission and absorption cross sections (see Fig. 7). The inversion point of the isothermal reactivity is extremely sensitive to the shape of the ^{235}U fission and capture cross sections.

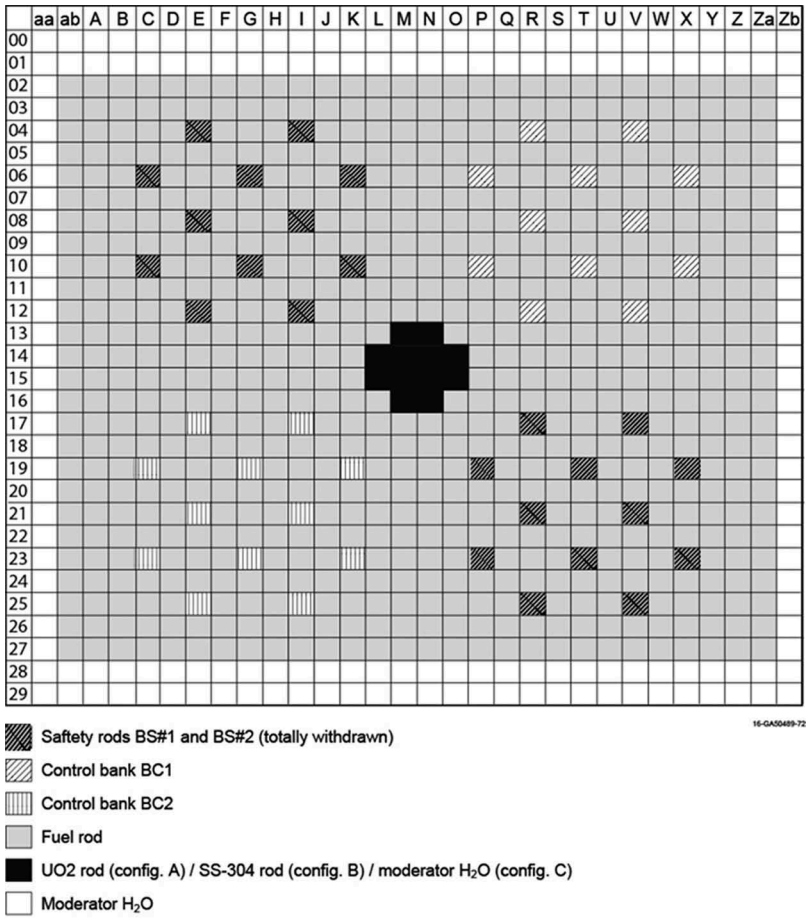

Fig. 6. Core configurations of the IPEN/MB-01 reactor considered in the benchmarks.

TABLE VI

Final Values for the Inversion Points of the Isothermal Reactivity Coefficient of the IPEN/MB-01 Reactor and Corresponding Total Uncertainties

Configuration A	Configuration B	Configuration C
14.99 ± 0.24°C	21.54 ± 0.24°C	22.36 ± 0.26°C

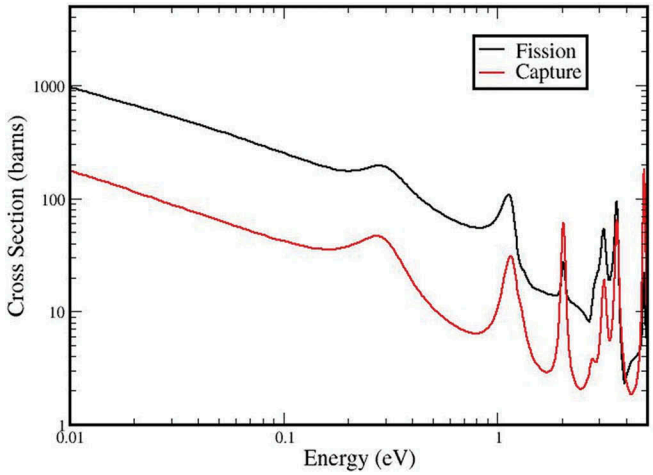

Fig. 7. The ^{235}U fission and capture cross section below 5 eV.

It should be pointed out that the IPEN reactor core is slightly under-moderated uranium-water lattice with a neutron spectrum with a corresponding average neutron lethargy causing fission (EALF) of about 0.2 eV as indicated in the International Criticality Safety Benchmark Evaluation Project (ICSBEP) Handbook.[20] This feature is confirmed by the fact that the water density contribution to the reactivity is negative in nominal conditions.[19] The hydrogen absorption represents a negligible effect due the under-moderated uranium-water lattice. In addition, the Doppler reactivity effect is also negative mainly due to the ^{238}U resonance capture.

III.C. Calculation Methodology

The inversion point of the isothermal reactivity coefficient of the IPEN/MB-01 is an interesting benchmark problem. Its theoretical treatment may vary depending on the judgment of a reactor physics specialist and on the available computational resources. The approach adopted here is to make k_{eff} calculations for a temperature range that covers the interval from the lowest to the highest temperature of the experimental data, keeping the control banks at their critical positions of 20°C in all the calculations. All physical quantities that have temperature dependence such as cross sections [Doppler effect and S(α, β)], material density (water for example), etc., must be taken into account in the analysis. Subsequently, the reactivity change due to the temperature variation relative to the 20°C can be calculated as

$$\rho_i = \frac{(k_i - k_{20})}{(k_i \cdot k_{20})} , \qquad (1)$$

where k_i is the k_{eff} for temperature T_i, and k_{20} is the k_{eff} at 20°C, respectively. The theoretical determination of the inversion point is based on the behavior of the reactivity change as a function of temperature. This reactivity shows a maximum value for which the temperature corresponds to the inversion point of the isothermal reactivity coefficient.

The theoretical analyses applied to the inversion point of the isothermal reactivity coefficient of the IPEN/MB-01 reactor were carried out in a deterministic approach employing the coupled systems NJOY/AMPX-II/TORT codes.[26] The NJOY code system[27] (version 2012.50) is used for the multigroup and pointwise cross-section generation, AMPX-II (Ref. 28) is used for the generation of the few-group weighting cross sections, and TORT (Ref. 29) [a three-dimensional (3-D_ S_N transport theory code] is used to calculate k_{eff} for the reactor core. The calculations were carried out in two ways: (1) using the entire ENDF/B-VII.0 (Ref. 30) as the basic nuclear data library, and (2) using the new ^{235}U evaluation, which is available at the Nuclear Data Bank of the Nuclear Energy Agency[31] with the remainder nuclides taken from ENDF/B-VII.0.

The calculation scheme used in the analyses is shown in Fig. 8. The thermal scattering law for hydrogen bound in water was obtained with the LEAPR module of NJOY. The nuclear data were generated in the interval from 4°C to 32°C in steps of 2°C.

The RECONR, BROADR, UNRESR, THERMR, and GROUPR modules of NJOY are used in order to reconstruct and to Doppler broaden the cross sections, to calculate the self-shielding effects in the unresolved resonance region, to build the scattering matrices in the thermal region, and to transform these data into multigroup parameters, respectively. The next step was the production of a set of broad group

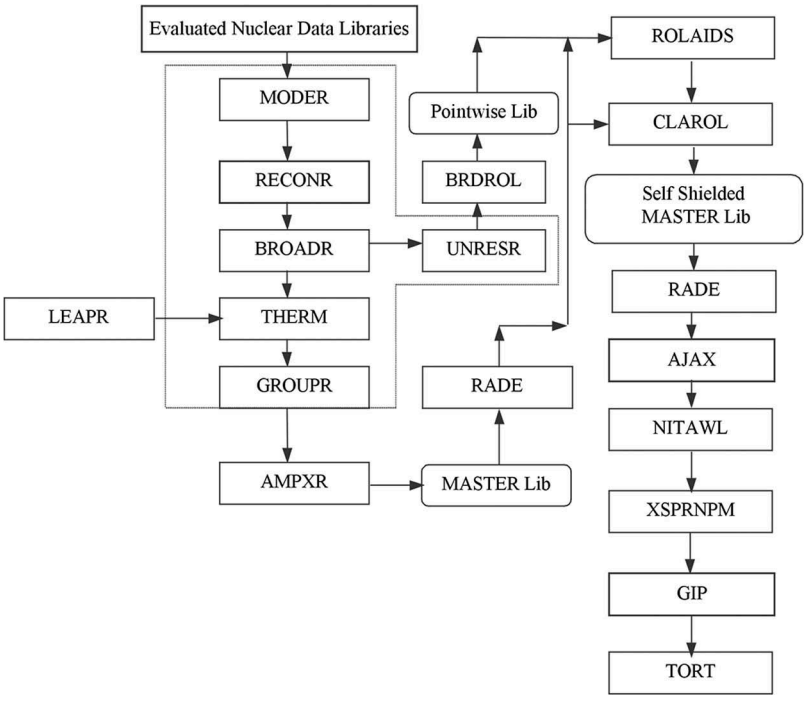

Fig. 8. Schematic diagram for the calculational methodology.

energy library using the AMPX-II package. The pointwise and fine multigroup cross sections produced in the previous step were transferred to AMPX-II by two in-house interface modules[25] called BRDROL and AMPXR. The self-shielding treatment in the resolved resonances was carried out by the ROLAIDS module of AMPX-II. The neutron spectra and subsequent cross section collapsing in the several regions of the IPEN/MB-01 reactor were carried out by XSDRNPM. The ROLAIDS module of AMPX-II employs the collision probability method considering pointwise cross sections and accounts for both space and energy self-shielding. The ROLAIDS method also considers the mutual shielding among the actinides present in the problem. XSDRNPM is a one-dimensional code and solves the transport equation using the S_N method. First, the XSDRNPM cell model considered an infinite array of fuel pin square cells. The k_{inf} spectral calculations were performed in a cylindrical geometry in the fine group structure considering a white boundary condition at the outer boundary of the cylindrized cell. The group cross sections for all nuclides were homogenized in a fine group level. Next, these data are merged with those of other regions such as radial, top and bottom reflectors, and so on. Finally, XSDRNPM considers radial and axial slices of the IPEN/MB-01 reactor to get the final spectra for the broad group collapsing. The broad group cross sections of the control rods, guide tube, and bottom plugs were obtained using a super-cell model. This set of fine multigroup libraries was collapsed to a set of broad groups. At this point, the cross-section library is problem dependent. The order of scattering (Legendre order expansion) was P_3 throughout the analysis. Finally, the broad group library is conveniently formatted to the TORT (3-D Discrete Ordinates Code) format using the GIP (Ref. 32) program. Subsequently, with the broad group cross-sections libraries previously generated, TORT performed k_{eff} calculations considering a fully 3-D geometric modeling of the IPEN/MB-01 reactor core.

The fully 3-D geometric setup for the TORT calculations was considered in the *X-Y-Z* geometry and P_3 approximation. The mesh distribution comprises 52 mesh intervals in *X* direction, 50 mesh intervals in *Y* direction, and 81 mesh intervals in *Z* direction, for a total of 210 600 intervals. These intervals are represented by 10 numbers of material zones. The boundary conditions considered were void at top and bottom and at the left and right borders of the problem. The convergence criterion for the criticality calculations was set to the 10^{-5} for the flux and the fission source and 10^{-6} for the eigenvalue.

As suggested in Ref. 19 the multigroup library for all nuclides that take part in the benchmark model was generated in 620 groups of energy. These data were collapsed in a structure of 16 groups with 5 thermal groups employing the XSDRNPM module of AMPX-II. TORT was run considering this broad group structure and $S_{16}P_3$. These were the group structure and S_N order to be used in the theoretical analyses of the inversion point of the isothermal reactivity coefficient of the IPEN/MB-01 reactor. A complete detail of the broad group library generation can be found in Ref. 19.

The whole pattern of calculations as shown in Fig. 8 (cross-section generation and subsequent TORT k_{eff} calculations) was considered for the entire temperature interval spanning from 4°C to 32°C. Equation (1) was employed for the determination of the reactivity variation as a function of the temperature. Finally, the NJOY/AMPX-II/TORT analyses follow all recommendations of Ref. 19.

In order to illustrate the results from the methodology NJOY/AMPX-II/TORT for the several temperatures considered in the analyses, Table VII shows k_{eff} and reactivities relative to the 20°C case for configuration A and ENDF/B-VII.0 library.

The reactivity as a function of the temperature was subsequently least-square fitted in a second order polynomial function as

$$\rho(T) = A_0 + A_1 T + A_2 T^2 \ , \qquad (2)$$

where $\rho(T)$ represents the reactivity at temperature T in °C, and A_k is the k'th polynomial coefficient. The expansion polynomial coefficients are shown in the Table VIII.

The corresponding covariance matrix for the polynomial coefficients ($\sigma_{A_i A_j}$) is shown in Table IX.

TABLE VII

Calculated k_{eff} and Reactivities Relative to the 20°C Case for Configuration A

Temperature (°C)	k_{eff}	Reactivity (pcm)
4.0	0.999465	5.41
6.0	0.999504	9.32
8.0	0.999549	13.84
10.0	0.999563	15.20
12.0	0.999558	14.72
14.0	0.999542	13.17
16.0	0.999519	10.86
18.0	0.999470	5.91
20.0	0.999411	0.00
22.0	0.999333	−7.84
24.0	0.999230	−18.08
26.0	0.999131	−28.02
28.0	0.999021	−39.03
30.0	0.998905	−50.69
32.0	0.998780	−63.21

TABLE VIII

Polynomial Coefficients for Configuration

A_0	−6.44569 ± 1.31080
A_1	3.87034 ± 0.16486
A_2	−0.17839 ± 0.0045

TABLE IX

Covariance Matrix for the Polynomial Coefficients

	A_0	A_1	A_2
A_0	1.71821	−0.20132	0.005
A_1	−0.20132	0.02718	−7.22E-04
A_2	0.005	−7.22E-04	2.01E-05

The inversion point can be determined as the maximum of Eq. (2):

$$T_{inv} = -\frac{A_1}{2A_2} . \tag{3}$$

The error propagation to the inversion point is given by

$$\sigma^2_{T_{inv}} = \left(\frac{\partial T_{inv}}{\partial A_1}\right)^2 \sigma^2_{A_1} + \left(\frac{\partial T_{inv}}{\partial A_2}\right)^2 \sigma^2_{A_2} + 2\left(\frac{\partial T_{inv}}{\partial A_1}\right)\left(\frac{\partial T_{inv}}{\partial A_2}\right)\sigma_{A_1A_2} , \tag{4}$$

with

$$\frac{\partial T_{inv}}{\partial A_1} = -\frac{1}{2A_2} \tag{5}$$

and

$$\frac{\partial T_{inv}}{\partial A_2} = \frac{A_1}{2A_2^2} , \tag{6}$$

and where σ_{A_1}, σ_{A_2}, and $\sigma_{A_1A_2}$ are the elements of the covariance matrix shown in Table IX. The uncertainty in the theoretical inversion point arises from the least squares approach. It is a property of the fitting data and the fitting function chosen to describe the phenomenon.

The final result for the inversion point and its corresponding uncertainty is obtained by applying Eqs. (3) through (6) and is equal to 10.85 ± 0.20°C (1σ). The calculation/experiment comparisons for configuration A are shown in a graphical form in Fig. 9.

The inversion point of the isothermal reactivity coefficient for configurations B and C were obtained in a similar approach. Figures 10 and 11 show the theory/experiment comparison for these configurations.

Tables X and XI summarize for ENDF/B-VII.0 and for the new ^{235}U evaluation, respectively, the theory-experiment comparison of the inversion point of the isothermal reactivity coefficient of the IPEN/MB-01 as well as the error on the isothermal reactivity coefficient. This last quantity is explained during the analyses of the theoretical and experimental data below. For clarity, the results shown in Tables X and XI for the (C-E)/E (%) are also displayed in Fig. 12.

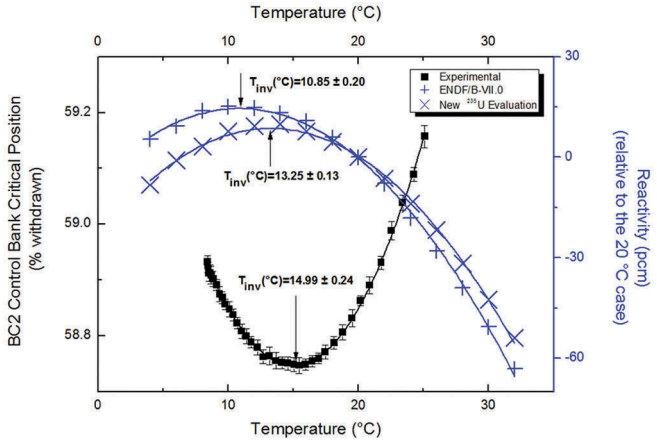

Fig. 9. Calculated reactivity variation and BC2 control bank critical position as a function of temperature for configuration A.

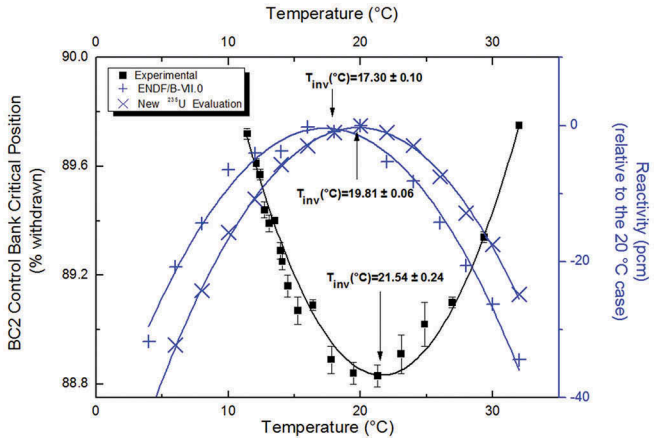

Fig. 10. Calculated reactivity variation and BC2 control bank critical position as a function of temperature for configuration B.

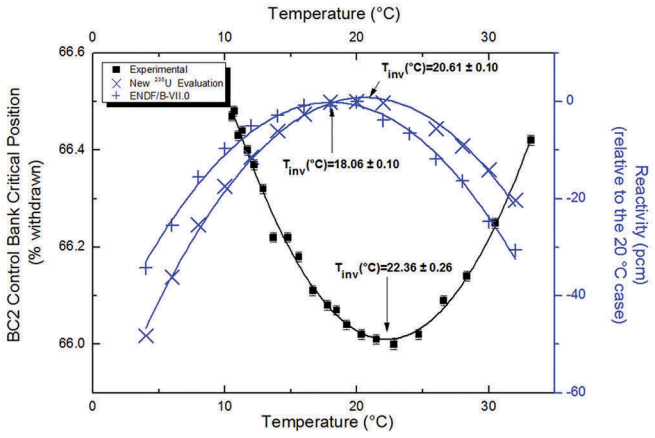

Fig. 11. Calculated reactivity variation and BC2 control bank critical position as a function of temperature for configuration C.

The differences for the inversion point (ΔT_{inv}), as shown in Tables X and XI are negative which is consistent with the underprediction of the calculated isothermal reactivity coefficient shown in previous works (see Refs. 18 and 19 for instance). This implies that the calculated reactivity coefficient is smaller than the experimental one. Furthermore, (ΔT_{inv}) shown in Tables X and XI within the uncertainty range of one σ are invariant for the three configurations considered in this work. This characteristic shows that the experiments, evaluation, and the theoretical analysis are consistent from configuration to configuration. There appears to be a systematic bias which might reside in the basic nuclear data utilized in the analyses. The largest difference from the experimental value is −4.30°C, which is shown in configuration C. At first glance there appears to be a considerable discrepancy in the theory/benchmark comparison. This discrepancy is well outside of the 3σ range of the benchmark uncertainty. However from the experimental curve of the isothermal reactivity coefficient of the IPEN/MB-01 reactor,[19] one may note that for every 1°C variation in the temperature scale there is a variation of nearly 0.416 ± 0.0031 pcm/°C in the reactivity coefficient. Therefore, for a variation of −4.30°C, there is a variation (or error) of −1.79 ± 0.12 pcm/°C in the isothermal reactivity coefficient (α_{iso}). This deviation is a considerable improvement from older evaluations which for a long time showed a systematic discrepancy of −5.0 pcm/°C (Ref. 33). Nonetheless, when the new nuclear data evaluation for ^{235}U is used the error in the reactivity coefficient determination is −0.73 ± 0.12 pcm/°C which attends the desired accuracy (−1.0 pcm/°C) (Ref. 34) for the calculation of the reactivity coefficient. In this aspect, the whole methodology and the nuclear data library considered in this work attain the desired accuracy for the determination of the isothermal reactivity coefficient. A good part of the improvements in the agreement between calculated and benchmark values for the isothermal reactivity coefficient is due to the incorporation of the new η-shape of ^{235}U (Ref. 35) in ENDF/B-VII.0 and in the new resonance parameters of the ^{235}U evaluation. For completeness and better understanding of this work, Tables X and XI contain the values of the variation or error of the isothermal reactivity coefficient due to the variation of the calculated inversion point relatively to the experimental values for all

TABLE X

Theory/Benchmark Comparison of the Inversion Point for ENDF/B-VII.0

ENDF/B-VII.0			
Calculated Inversion Point (°C)	(C-E)/E ± (1σ) (%)	ΔT_{inv} (°C)	$\alpha_{isoerror}$ (pcm/°C)
Configuration A Benchmark Value = 14.99 ± 0.24 (°C)			
10.85 ± 0.20	−27.65 ± 1.80	−4.15 ± 0.32	−1.72 ± 0.13
Configuration B Benchmark Value = 21.54 ± 0.24 (°C)			
17.30 ± 0.10	−19.69 ± 1.00	−4.24 ± 0.26	−1.76 ± 0.11
Configuration C Benchmark Value = 22.36 ± 0.26 (°C)			
18.06 ± 0.10	−19.23 ± 1.05	−4.30 ± 0.28	−1.79 ± 0.12

TABLE XI

Theory/Benchmark Comparison of the Inversion Point for ENDF/B-VII.0 and the New ^{235}U Evaluation

New ^{235}U Evaluation with Others from ENDF/B-VII.0			
Calculated Inversion Point (°C)	(C-E)/E ± (1σ) (%)	ΔT_{inv} (°C)	$\alpha_{isoerror}$ (pcm/°C)
Configuration A Benchmark Value = 14.99 ± 0.24 (°C)			
13.25 ± 0.12	−11.63 ± 1.65	−1.74 ± 0.27	−0.73 ± 0.11
Configuration B Benchmark Value = 21.54 ± 0.24 (°C)			
19.81 ± 0.06	−8.04 ± 1.05	−1.73 ± 0.26	−0.72 ± 0.10
Configuration C Benchmark Value = 22.36 ± 0.26 (°C)			
20.61 ± 0.10	−7.86 ± 1.15	−1.76 ± 0.28	−0.73 ± 0.12

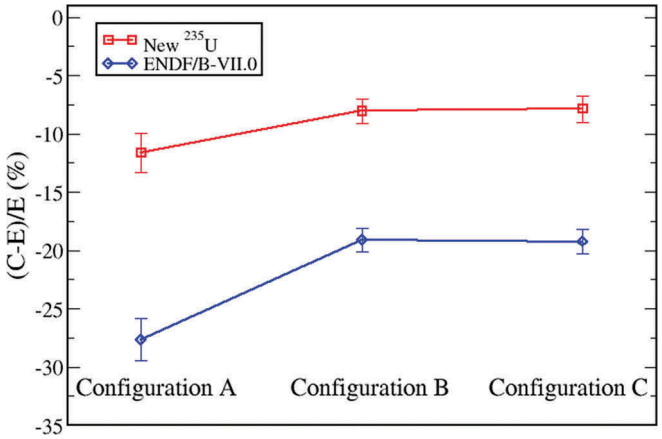

Fig. 12. Graphical representation of the percentage (C-E)/E of the inversion temperatures.

three configurations considered in this evaluation. Finally, the isothermal reactivity errors found in this work are consistent with previous work (Ref. 19) which shows a maximum error of −0.90 ± 0.05 pcm/°C considering ENDF/B-VI.8 (Ref. 36). In this aspect, the experiments and evaluation of the inversion point of the isothermal reactivity coefficient of the IPEN/MB-01 reactor show consistency and completeness.

IV. CONCLUSIONS

Re-evaluation of the ^{235}U resonance parameter has been performed to address issues with standard fission cross-section values in the resolved resonance region. The experimental data entered in the evaluation are well represented and the standard values are reproduced. The present work demonstrates that the ^{235}U resonance evaluation in the thermal range represents an improvement compared to previous ^{235}U resonance evaluations in existing cross-section libraries. The benchmark calculations were carried out by taking into account the IPEN/MB-01 benchmark evaluation recently approved for inclusion in the IRPhE handbook, which has been found to be extremely helpful to test the ^{235}U nuclear data for thermal reactor applications. The reactor evaluated quantity used in the calculations is the inversion point of the isothermal reactivity coefficient of the IPEN/MB-01 reactor. This quantity showed to be very sensitive to the ^{235}U nuclear data, mainly to the shape of η(E). The analyses revealed that there is a considerable improvement in theory/experiment predictions when the new ^{235}U resonance parameters are considered in the analyses. The maximum error in the prediction of the isothermal reactivity is −0.73 ± 0.12 pcm/°C, which is within the desired accuracy of the determination of this integral response.

References

1. G. DE SAUSSURE et al., "A New Resonance Region Evaluation of Neutron Cross-Sections for ^{235}U," *Nucl. Sci. Eng.*, **103**, 109 (1989); http://dx.doi.org/10.13182/NSE89-A28500.

2. N. M. LARSON, "Updated Users' Guide for SAMMY: Multi-Level R-Matrix Fits to Neutron Data Using Bayes's Equations," ENDF-364/R2, Oak Ridge National Laboratory, (2008), available at Radiation Safety Information Computational Center (RSICC) as PSR-158.

3. S. CATHALAU et al., "Qualification of the JEF2.2 Cross Sections in the Epithermal and Thermal Energy Ranges Using a Statistical Approach," *Nucl. Sci. Eng.*, **121**, 326 (1995); http://dx.doi.org/10.12182/NSE95-A28568.

4. L. C. LEAL et al., "R-Matrix Analysis of ^{235}U Neutron Transmission and Cross-Section Measurements in the 0- to 2.25-keV Energy Range," *Nucl. Sci. Eng.*, **131**, 230 (1999); http://dx.doi.org/10.13182/NSE99-A2031.

5. M. FUKUSHIMA et al., "Benchmark Models for Criticalities of FCA-IX Assemblies with Systematically Changed Neutron Spectra," *J. Nucl. Sci. Technol.*, **53**, 406 (2015); http://dx.doi.org/10.1080/00223131.2015.1054911.

6. "Final Report of WPEC Subgroup 29 on ^{235}U Capture Cross-Section in the keV to MeV Energy Region", NEA/NSC/WPEC/DOC(2011)433, Nuclear Energy Agency, Organization for Economic Co-operation and Development (2011).

7. Y. DANON, "Nuclear Data Measurements at RPI," presented at 2011 Cross Section Evaluation Working Group Mtg., National Nuclear Data Center, Brookhaven National Laboratory, Upton, New York, November 16, 2011.

8. T. A. JANDEL et al., "New Precision Measurements of the ^{235}U(n,γ) Cross Section," *Phys. Rev. Lett.*, **109**, 202506 (2012); http://dx.doi.org/10.1103/PhysRevLett.109.202506.

9. L. ERRADI, A. SANTAMARINA, and O. LITAIZE, "The Reactivity Temperature Coefficient Analysis in Light Water Moderated UO_2 and UO_2-PuO_2 Lattices," *Nucl. Sci. Eng.*, **144**, 47 (2003); http://dx.doi.org/10.13182/NSE144-47.

10. J. A. HARVEY et al., "High-Resolution Neutron Transmission Measurements on ^{235}U, ^{239}Pu, and ^{238}U," *Proc. Int. Conf. Nuclear Data for Science and Technology*, Mito, Japan, May 30–June 3, 1988.

11. Neutron Cross Section Standards and References, International Atomic Energy Agency (2015); https://www-nds.iaea.org/standards/ (accessed January 23, 2017).

12. R. R. SPENCER et al., "Parameters of the 1.056-eV Resonance in ^{240}Pu and the 2200 m/s Neutron Total Cross Sections of ^{235}U, ^{239}Pu, and ^{240}Pu," *Nucl. Sci. Eng.*, **96**, 318 (1987); http://dx.doi.org/10.13182/NSE87-A16395.

13. C. PARADELA et al., "High Accuracy ^{235}U(n,f) Data in the Resonance Region," *Eur. Phys. J.*, **111** (2016); https://doi.org/10.1051/epjconf/201611102003. See also *WONDER-2015 4th Int. Workshop Nuclear Data Evaluation for Reactor Application*, Aix-en-Provence, France, October 5–8, 2015.

14. L. W. WESTON and J. H. TODD, "High-Resolution Fission Cross-Section Measurements of ^{235}U and ^{239}U," *Nucl. Sci. Eng.*, **111**, 415 (1992); http://dx.doi.org/10.13182/NSE92-A15488.

15. R. B. PEREZ, G. DE SAUSSURE, and E. G. SILVER, "Simultaneous Measurements of the Neutron Fission and Capture Cross Sections for Uranium-235 for Neutron Energies from 8 eV to 10 keV," *Nucl. Sci. Eng.*, **52**, 46 (1973); http://dx.doi.org/10.13182/NSE73-A23288.

16. M. S. MOORE et al., "Spin Determination of Resonance Structure in (^{235}U + n) Below 25 keV," *Phys. Rev. C*, **18**, *3*, 1328 (1978); https://doi.org/10.1103/PhysRevC.18.1328.

17. A. DOS SANTOS et al., "The Inversion Point of the Isothermal Reactivity Coefficient of the IPEN/MB-01 Reactor," IPEN (MB01)-LWR-COEF-KINRESR-001, approved for publication in *International Handbook of Evaluated Reactor Physics Benchmark Experiments*, p. 1, NEA/NSC, Paris (Mar. 2017).

18. A. DOS SANTOS, "Some ENDF/B-VI Benchmark Results," *Trans. Am. Nucl. Soc.*, **76**, 332 (1997).

19. A. DOS SANTOS et al., "The Inversion Point of the Isothermal Reactivity Coefficient of the IPEN/MB-01 Reactor—II: Theoretical Analysis," *Nucl. Sci. Eng.*, **151**, 237–50 (2005); http://dx.doi.org/10.13182/NSE05-A2543.

20. A. DOS SANTOS et al., "LEU-COMP-THERM-077: Critical Loading Configurations of the IPEN/MB-01 Reactor," *International Handbook of Evaluated Criticality Safety Benchmark Experiments*, J. B. BRIGGS, Ed., NEA/NSC/DOC (95)03/I, Paris (Sep. 2004).

21. A. DOS SANTOS et al., "LEU-COMP-THERM-044: Critical Loading Configurations of the IPEN/MB-01 Reactor with UO_2, Stainless Steel And Copper Rods," *International Handbook of Evaluated Criticality Safety Benchmark Experiments*, J. B. BRIGGS, Ed., NEA/NSC/DOC (95)03/I, Paris (Sep. 2008).

22. A. DOS SANTOS et al., "IPEN (MB01)-LWR-COEF-KIN-RESR-001: Reactor Physics Experiments in the IPEN/MB-01 Research Reactor Facility," *International Handbook of Evaluated Reactor Physics Benchmark Experiments*, p. 1, NEA/NSC, Paris (2012).

23. A. DOS SANTOS et al., "The Inversion Point of the Isothermal Reactivity Coefficient of the IPEN/MB-01 Reactor—I: Experimental Procedure," *Nucl. Sci. Eng.*, **133**, 314 (1999); http://dx.doi.org/10.13182/NSE99-A2091.

24. A. DOS SANTOS et al., "New Experimental Results for the Inversion Point of the Isothermal Reactivity Coefficient of the IPEN/MB-01 Reactor," *Ann. Nucl. Energy*, **36**, 1740 (2009); https://doi.org/10.1016/j.anucene.2009.08.015.

25. V. TURCHIN, *Slow Neutrons, Israel Program for Scientic Translations*, Sivan Press, Jerusalem (1965) (Russian Original), Gosatomizdat, Moscow (1963).

26. A. DOS SANTOS et al., "Criticality Analysis Based on the Coupled NJOY/AMPX-II/TORT Systems," *Proc. Int. Conf. Physics of Nuclear Science and Technology*, Pittsburgh,

Pennsylvania, May 7–12, 2000, American Nuclear Society (2000).

27. R. E. MacFARLANE, D. W. MUIR, and R. M. BOUICORT, "NJOY—Code System for Producing Pointwise and Multigroup Neutron and Photon Cross Sections from ENDF Data," LA-12740-M, Los Alamos National Laboratory (Oct. 1994).
28. N. M. GREENE et al., "AMPX-II: A Modular Code System for Generating Coupled Multigroup Neutron-Gamma Libraries from ENDF/B," ORNL-TM-3706 (1976).
29. W. A. RHOADES and D. B. SIMPSON, "The TORT Three-Dimensional Discrete Ordinates Neutron/Photon Transport Code (TORT Version 3)," ORNL/TM-13221 (1991).
30. O. OBLOZINSKY. and M. HERMAN, "Special Issue on Evaluated Nuclear Data File ENDF/B-VII.0," *Nucl. Data Sheets*, **107**, *12* (2006).
31. R. ICHOU et al., "Use of Integral Experiments to Test a New ^{235}U Evaluation for the CIELO Project," *Proc. PHYSOR 2016*, Sun Valley, Idaho, May 1–5, 2016.
32. W. A. RHOADES, "The GIP Program for Preparation of Group-Organized Cross Section Libraries," Oak Ridge National Laboratory (1975).
33. J. R. ASKEW, F. J. FAYES, and W. N. FOX, "Thermal Reactor Temperature Coefficient Studies in the United Kingdom," AEEW-R-886 (1973).
34. J. BOUCHARD, C. GOLINELLI, and H. TELLIER, "Besoins En Données Nucléaires Pour Les Réacteurs À Neutrons Thermiques," *Proc. Int. Conf. Nuclear Data for Science and Technology*, Dordrecht, Netherlands, September 6–10, 1982, Vol. 1072, p. 21 (1983).
35. H. WEIGMANN et al., "Measurements of H of ^{235}U for Subthermal Neutron Energies," *Proc. Conf. Physics of Reactors: Operation, Design, and Computation, PHYSOR-90*, Marseille, France, April 23–26, Vol. 3, p. 33 (1990).
36. "ENDF/B-VI Summary Documentation," BNL-NCS-17541 (ENDF-201), P. F. ROSE, Ed., Part 4, (ENDF/B-VI), National Nuclear Data Center, Brookhaven National Laboratory (Release-8 2002) (2002).
37. R. GWIN et al., "Measurements of the Neutron Fission Cross Sections of ^{235}U (E_n = 0.01 eV to 30 keV) and ^{239}Pu (E_n = 0.01 to 60 eV)," *Nucl. Sci. Eng.*, **88**, 37 (1984); http://dx.doi.org/10.13182/NSE84-A17138.
38. L. W. WESTON and J. H. TODD, "Subthreshold Fission Cross Section of ^{240}Pu and the Fission Cross Sections of ^{235}U and ^{239}Pu," *Nucl. Sci. Eng.*, **88**, 567 (1984); http://dx.doi.org/10.13182/NSE84-A18373.
39. C. WAGEMANS et al., "Subthermal Fission Cross Section Measurements for ^{235}U and ^{239}Pu," *Nuclear Data for Science and Technology*, p. 91, Mito, Japan (1988).
40. J. A. WARTENA, H. WEIGMANN, and C. BURKHOLZ, IAEA TECDOC 941, p. 123 (1987).
41. G. DE SAUSSURE et al., "Simultaneous Measurements of the Neutron Fission and Capture Cross Section for ^{235}U for Incident Neutron Energy from 0.4 eV to 3 keV," ORNL/TM-1804, Martin Marietta Energy Systems, Inc., Oak Ridge National Laboratory (1967).